The Journal of Neuroscience, November 1, 1998, *18*(21):9099–9111

Spike-and-Wave Oscillations Based on the Properties of $GABA_B$ Receptors

Alain Destexhe

Neurophysiology Laboratory, Department of Physiology, Laval University, Québec G1K 7P4, Canada

Neocortical and thalamic neurons are involved in the genesis of generalized spike-and-wave (SW) epileptic seizures. The cellular mechanism of SW involves complex interactions between intrinsic neuronal firing properties and multiple types of synaptic receptors, but because of the complexity of these interactions the exact details of this mechanism are unclear. In this paper these types of interactions were investigated by using biophysical models of thalamic and cortical neurons. It is shown first that, because of the particular activation properties of $GABA_B$ receptor-mediated responses, simulated field potentials can display SW waveforms if cortical pyramidal cells and interneurons generate prolonged discharges in synchrony, without any other assumptions. Here the "spike" component coincided with the synchronous firing, whereas the "wave" component was generated mostly by slow $GABA_B$-mediated K^+ currents. Second, the model suggests that intact thalamic circuits can be forced into a ~3 Hz oscillatory mode by corticothalamic feedback. Here again, this property was attributable to the characteristics of $GABA_B$-mediated inhibition. Third, in the thalamocortical system this property can lead to generalized ~3 Hz oscillations with SW field potentials. The oscillation consisted of a synchronous prolonged firing in all cell types, interleaved with a ~300 msec period of neuronal silence, similar to experimental observations during SW seizures. This model suggests that SW oscillations can arise from thalamocortical loops in which the corticothalamic feedback indirectly evokes $GABA_B$-mediated inhibition in the thalamus. This mechanism is shown to be consistent with a number of different experimental models, and experiments are suggested to test its consistency.

Key words: computational models; thalamus; cerebral cortex; epilepsy; absence; intrinsic properties; low-threshold spikes; spindle oscillations; thalamocortical

Generalized spike-and-wave (SW) patterns characterize the human electroencephalogram during several types of epilepsy as well as in animal models of absence seizures. Initially suggested by Jasper and Kershman (1941), the possible involvement of the thalamus in SW seizures was shown by recordings of thalamic nuclei in humans during absence attacks (Williams, 1953; Prevett et al., 1995). An important role for the thalamus also is supported by electrophysiological recordings in experimental models of SW seizures, which show that cortical and thalamic cells fire prolonged discharges in phase with the "spike" component, whereas the "wave" is characterized by a silence in all cell types (Pollen, 1964; Steriade, 1974; Avoli et al., 1983; McLachlan et al., 1984; Buzsáki et al., 1990; Inoue et al., 1993). Electrophysiological recordings also indicate that spindle oscillations, which are generated by thalamic circuits (Steriade et al., 1990, 1993), can be transformed gradually into SW discharges, and all manipulations that promote or antagonize spindles have the same effect on SW (Kostopoulos et al., 1981a,b; McLachlan et al., 1984). Finally, it has been demonstrated that SW patterns disappear after thalamic lesions or after inactivation of the thalamus (Pellegrini et al., 1979; Avoli and Gloor, 1981; Vergnes and Marescaux, 1992).

A series of pharmacological results suggests that $GABA_B$ receptors play a critical role in the genesis of SW discharges in rats, because $GABA_B$ agonists exacerbate seizures whereas $GABA_B$ antagonists suppress them (Hosford et al., 1992; Snead, 1992; Puigcerver et al., 1996; Smith and Fisher, 1996). The anti-absence drug clonazepam seems to act by diminishing $GABA_B$-mediated IPSPs in thalamocortical (TC) cells, reducing their tendency to burst in synchrony (Huguenard and Prince, 1994a; Gibbs et al., 1996). In ferret thalamic slices, spindle oscillations can be transformed into slower ~3 Hz oscillations after blocking $GABA_A$ receptors, and, like SW, these oscillations are suppressed by $GABA_B$ receptor antagonists (von Krosigk et al., 1993). These experiments could be replicated by computational models of thalamic circuits (Destexhe and Sejnowski, 1995; Destexhe et al., 1996a; Golomb et al., 1996).

Although these results could suggest a thalamic origin of SW seizures involving $GABA_B$-mediated mechanisms, clear evidence suggests a determinant role for the cortex: thalamic injections of high doses of $GABA_A$ antagonists such as penicillin (Ralston and Ajmone-Marsan, 1956; Gloor et al., 1977) or bicuculline (Steriade and Contreras, 1998) led to 3–4 Hz oscillations, with no sign of SW discharge. On the other hand, injection of the same drugs to the cortex, with no change in the thalamus, resulted in seizure activity with SW patterns (Gloor et al., 1977; Steriade and Contreras, 1998).

These experiments show that both cortical and thalamic neurons are necessary to generate SW rhythms and that both $GABA_A$ and $GABA_B$ receptors are actively involved, but the exact mechanisms are unclear. In this paper a thalamocortical loop mechanism for the genesis of SW oscillatory patterns was investigated by the use of computational models that were based on the complex intrinsic firing properties of thalamic and cortical neurons (see Llinás, 1988) and the properties particular to each receptor type (Destexhe et al., 1998b).

Received June 15, 1998; revised Aug. 13, 1998; accepted Aug. 17, 1998.

This research was supported by the Medical Research Council of Canada (MT-13724). We thank D. Contreras and N. Kopell for comments on this manuscript.

Correspondence should be addressed to Dr. Alain Destexhe at the above address.

 0270-6474/98/189099-13$05.00/0

MATERIALS AND METHODS

All models that are shown here were based on biophysical representations of the ionic mechanisms underlying synaptic currents, field potential generation, intrinsic firing properties, and network behavior. The modeling methods that were used to simulate these various aspects are described successively.

Synaptic currents. Postsynaptic currents mediated by glutamate AMPA and NMDA receptors as well as by GABAergic $GABA_A$ and $GABA_B$ receptors were simulated by kinetic models of postsynaptic receptors (Destexhe et al., 1994, 1998b). When a spike occurred in the presynaptic cell, a brief pulse of transmitter concentration (0.5 mM during 0.3 msec) was simulated in the synaptic cleft, and binding of the transmitter to postsynaptic receptors occurred according to simple open/closed kinetics, leading to a transient increase of the postsynaptic current described by the following equation (Destexhe et al., 1994):

$$I_{syn} = \bar{g}_{syn}\, m\, (V - E_{syn}) \text{ and} \tag{1}$$

$$\frac{dm}{dt} = \alpha\, [T]\, (1 - m) - \beta\, m, \tag{2}$$

where I_{syn} is the postsynaptic current, $\bar{g}_{syn}$ is the maximal conductance, m is the fraction of open receptors, E_{syn} is the reversal potential, $[T]$ is the transmitter concentration in the cleft, and α and β are forward and backward binding rate constants of T to open the receptors. This scheme was used to simulate AMPA, NMDA, and $GABA_A$ types of receptors, with the following parameters: $E_{syn} = 0$ mV, $\alpha = 0.94 \times 10^6\, M^{-1}\, s^{-1}$, $\beta = 180\, s^{-1}$ for AMPA receptors; $E_{syn} = 0$ mV, $\alpha = 11 \times 10^4\, M^{-1}\, s^{-1}$, $\beta = 6.6\, s^{-1}$ for NMDA receptors; and $E_{syn} = -80$ mV, $\alpha = 20 \times 10^6\, M^{-1}\, s^{-1}$, $\beta = 160\, s^{-1}$ for $GABA_A$ receptors. These parameters were obtained by fitting the model to postsynaptic currents recorded experimentally (see Destexhe et al., 1998b). In addition, NMDA receptors had a voltage-dependent term corresponding to an extracellular Mg^{2+} concentration of 2 mM [Jahr and Stevens (1990); see Destexhe et al. (1998b) for the details of implementation].

The modeling of slow $GABA_B$ receptor-mediated inhibition required a more complex scheme to capture the nonlinear properties of this type of interaction (Destexhe and Sejnowski, 1995). The activation properties of $GABA_B$ receptors were based on the following steps: (1) the binding of GABA on the $GABA_B$ receptor, leading to the activated receptor; (2) the activated $GABA_B$ receptor catalyzes the activation of G-proteins in the intracellular side; (3) the binding of activated G-proteins to open K^+ channels. These steps are described by the following equations:

$$I_{GABA_B} = \bar{g}_{GABA_B}\, \frac{s^n}{s^n + K_D}\, (V - E_K), \tag{3}$$

$$\frac{dr}{dt} = K_1\, [T]\, (1 - r) - K_2\, r, \text{ and} \tag{4}$$

$$\frac{ds}{dt} = K_3\, r - K_4\, s, \tag{5}$$

where $[T]$ is the GABA concentration in the synaptic cleft, r is the fraction of $GABA_B$ receptors in the activated form, s is the normalized G-protein concentration in activated form, $\bar{g}_{GABA_B}$ is the maximal postsynaptic conductance of K^+ channels, K_D is the dissociation constant of G-protein binding on K^+ channels, V is the postsynaptic membrane potential, and E_K is the equilibrium potential for K^+. The fitting of this model to experimental $GABA_B$ responses led to the following values of parameters (Destexhe et al., 1998b): $K_D = 100$, $K_1 = 9 \times 10^4\, M^{-1}\, s^{-1}$, $K_2 = 1.2\, s^{-1}$, $K_3 = 180\, s^{-1}$, and $K_4 = 34\, s^{-1}$, with $n = 4$ binding sites.

Field potentials. Extracellular field potentials were calculated from postsynaptic currents in single-compartment models according to the model of Nunez (1981):

$$V_{ext} = \frac{R_e}{4\pi} \sum_j \frac{I_j}{r_j}, \tag{6}$$

where V_{ext} is the electrical potential at a given extracellular site, $R_e = 230$ Ωcm is the extracellular resistivity, I_j is the postsynaptic current, and r_j is the distance between the site of generation of I_j and the extracellular site.

Field potentials were calculated from a single cell receiving 200 simulated synapses (100 excitatory synapses had AMPA and NMDA receptor types, and 100 inhibitory synapses had $GABA_A$ and $GABA_B$ receptors; see the scheme in Fig. 1*B*). In this case, trains of presynaptic action potentials were generated individually for each synapse. To avoid possible artifactual effects because of the coincident timing of action potentials at different synapses, a random time jitter of ±1 msec was included in the timing of each presynaptic action potential.

Intrinsic currents. Intrinsic voltage-dependent or calcium-dependent currents were modeled by kinetic models of the Hodgkin and Huxley (1952) type. These intrinsic membrane currents were described by the following generic equation:

$$I_{int} = \bar{g}_{int}\, m^N h^M\, (V - E_{int}), \tag{7}$$

$$\frac{dm}{dt} = \alpha_m\, (1 - m) - \beta_m\, m, \text{ and} \tag{8}$$

$$\frac{dh}{dt} = \alpha_h\, (1 - h) - \beta_h\, h, \tag{9}$$

where I_{int} is the intrinsic membrane current, $\bar{g}_{int}$ is the maximal conductance, and E_{int} is the reversal potential. The gating properties of the current were dependent on N activation gates and M inactivation gates, with m and h representing the fraction of gates in open form, and with respective rate constants α_m, β_m, α_h, and β_h. Rate constants were dependent on either membrane voltage (V) or intracellular calcium concentration.

Thalamocortical networks. Network models were based on single-compartment representations of thalamic and cortical neurons. The thalamocortical network was simulated with four cell types: cortical pyramidal cells (PY), cortical interneurons (IN), thalamic reticular cells (RE), and thalamocortical (TC) cells. Cortical cells represent layer VI of the cerebral cortex, in which PY cells constitute the major source of corticothalamic fibers. Because corticothalamic PY cells receive a significant proportion of their excitatory synapses from ascending thalamic axons (Hersch and White, 1981; White and Hersch, 1982), these cells mediate a monosynaptic excitatory feedback loop (thalamus–cortex–thalamus) that has been modeled here. Each layer of cells has been arranged in one dimension (connectivity is schematized in Fig. 4*A*). This one-dimensional network model with four cell types is a greatly simplified representation of the multilayered structure of the thalamocortical system, but no additional complexity was required.

The cellular models had intrinsic and synaptic currents described by the membrane equation:

$$C_m \dot{V}_i = -g_L\, (V_i - E_L) - \sum_j I_{int}^{ii} - \sum_k I_{syn}^{ki}, \tag{10}$$

where V_i is the membrane potential, $C_m = 1\ \mu F/cm^2$ is the specific capacity of the membrane, g_L is the leakage conductance, and E_L is the leakage reversal potential. Intrinsic and synaptic currents are represented by I_{int}^{ii} and I_{syn}^{ki}, respectively.

The synaptic currents I_{syn}^{ki}, from presynaptic cell k to postsynaptic cell i, were simulated by activating a short pulse of transmitter when cell k fired an action potential (see above). The receptor types present in synaptic connections between cells depended on the cell type. All excitatory connections (TC→RE, TC→IN, TC→PY, PY→PY, PY→IN, PY→RE, PY→TC) were mediated by AMPA receptors; some inhibitory connections (RE→TC, IN→PY) were mediated by a mixture of $GABA_A$ and $GABA_B$ receptors, whereas intra-RE connections were mediated by $GABA_A$ receptors. Simulations also were performed with NMDA receptors added to all excitatory connections (with maximal conductance set to 25% of that of AMPA), and no appreciable difference was observed. They therefore were not included in the present figures. The total synaptic conductance on each neuron was the same for cells of the same type and was expressed as the sum over all individual synaptic conductances of the same connection type. The total conductances corresponding to the reference state, displaying spindle oscillations, were 0.2 μS (AMPA, TC→RE), 0.2 μS ($GABA_A$, RE→RE), 0.02 μS ($GABA_A$, RE→TC), 0.04 μS ($GABA_B$, RE→TC), 0.6 μS (AMPA, PY→PY), 0.2 μS (AMPA, PY→IN), 0.15 μS ($GABA_A$, IN→PY), 0.03 μS ($GABA_B$, IN→PY), 1.2 μS (AMPA, PY→RE), 0.01 μS (AMPA, PY→TC), 1.2 μS (AMPA, TC→PY), and 0.4 μS (AMPA, TC→IN).

The connectivity between thalamic and cortical layers was topographic: within the thalamus and within cortex, each axon contacted the 11 nearest neighbors to the presynaptic cell. The axonal divergence was of 21 cells for projections between thalamus and cortex. The connection

topology, values of synaptic conductances, and robustness of the network were described in detail in a previous study (Destexhe et al., 1998a).

All intrinsic membrane currents I_{int}^{i} were described by a variant of the Hodgkin and Huxley (1952) model (Eqs. 7–9). All cell types had Na^+ and K^+ currents for generating action potentials, for which the kinetics was taken from Traub and Miles (1991). Additional currents conferred to each cell type the most salient features of its intrinsic firing patterns. Thalamic cells produced bursts of action potentials because of the presence of a T-current (see *inset* in Fig. 3*A*). In TC cells, in addition to I_T, the presence of I_h conferred oscillatory properties. The upregulation of I_h by intracellular Ca^{2+} led to waxing and waning properties of these oscillations, as detailed in previous models (Destexhe et al., 1993, 1996a, 1998a). In RE cells the T-current was of slower kinetics, as modeled previously (Destexhe et al., 1996b). Models for cortical cells were kept as simple as possible to reproduce their repetitive firing properties (see *inset* in Fig. 4*A*). IN cells contained no other current than was necessary for action potentials, producing similar firing patterns to "fast-spiking" cells (Connors and Gutnick, 1990). PY cells had one additional slow voltage-dependent K^+ current (I_M) generating adapting trains of action potentials, similar to "regular-spiking" pyramidal cells (Connors and Gutnick, 1990). The conductance values and the activation properties of all intrinsic membrane currents were identical to a previous study (Destexhe et al., 1998a).

Field potentials were calculated from network simulations. In this case only cortical pyramidal cells were considered and were arranged equidistantly in one dimension (intercellular distance of 20 μm). Then field potentials at a given extracellular site were calculated from postsynaptic currents:

$$V_{ext} = \frac{R_e}{4\pi} \sum_{i,k} \frac{I_{syn}^{ki}}{r_i}, \qquad (11)$$

where r_i is the distance between each PY cell and the extracellular site.

In some cases the contribution of the voltage-dependent current I_M in field potentials was evaluated according to the relation:

$$V_{ext} = \frac{R_e}{4\pi} \sum_{i} \frac{(I_M^i + \Sigma_k I_{syn}^{ki})}{r_i}, \qquad (12)$$

where I_M^i is the voltage-dependent K^+ current responsible for adaptation of repetitive firing in the ith PY cells.

All models were simulated by using NEURON (Hines and Carnevale, 1997) and were run on a Sparc-20 workstation (Sun Microsystems, Mountain View, CA).

RESULTS

The mechanism underlying a slow oscillation similar to SW is explained in three steps: (1) the nonlinear activation properties of $GABA_B$ responses can lead to the generation of SW waveforms in field potentials; (2) intact thalamic circuits can be forced into a ~3 Hz oscillation by corticothalamic feedback; (3) the combination of these two factors can generate ~3 Hz oscillations with SW field potentials in thalamocortical networks. These points are considered successively.

The nonlinear activation properties of $GABA_B$ responses

A property consistently observed for $GABA_B$ responses is that they require high stimulus intensities to be evoked, as shown in hippocampal (Dutar and Nicoll, 1988; Davies et al., 1990) and thalamic slices (Kim et al., 1997). This property can be reproduced under certain nonlinearity assumptions in the G-protein transduction mechanisms evoked by $GABA_B$ receptors; assuming that the binding of four G-proteins is required to activate K^+ channels is enough to provide a nonlinear stimulus dependence similar to $GABA_B$ responses (Destexhe and Sejnowski, 1995). The multiplicity of binding sites of G-proteins is indeed in agreement with the tetrameric structure of K^+ channels (Hille, 1992) and the cooperativity evidenced in the activation of $GABA_B$ responses (Sodickson and Bean, 1996).

The nonlinear stimulus dependence in the model of $GABA_B$ currents is illustrated in Figure 1*A*. An isolated presynaptic spike could not evoke detectable $GABA_B$ current (Fig. 1*A1*), in agreement with the absence of $GABA_B$-mediated miniature events (Otis and Mody, 1992; Thompson and Gahwiler, 1992; Thompson, 1994). However, a burst of 5–10 high-frequency spikes is a very powerful means of evoking $GABA_B$ responses (Fig. 1*A2*). The latter feature is consistent with the observation that $GABA_B$ responses appear only under high-intensity stimulus conditions (Dutar and Nicoll, 1988; Davies et al., 1990) and the evidence that bursts of high-frequency action potentials are an ideal presynaptic signal to evoke $GABA_B$ currents (Huguenard and Prince, 1994b; Kim et al., 1997). In the model this property is obtained from the fact that a sufficient level of G-proteins must be accumulated to evoke significant K^+ current.

Possible role of $GABA_B$-mediated currents in generating spike-and-wave field potentials

The possible role of the particular activation properties of $GABA_B$ currents in generating SW patterns was investigated by simulating field potentials from the postsynaptic currents generated by 100 excitatory synapses (AMPA and NMDA receptors) and 100 inhibitory synapses ($GABA_A$ and $GABA_B$ receptors; see scheme in Fig. 1*B* and Materials and Methods). With presynaptic trains consisting of single spikes, the voltage showed mixed EPSP/IPSP sequences, and the field potential was dominated by negative deflections (Fig. 1*C1*). By contrast, bursts of high-frequency presynaptic spikes produced mixed EPSP/IPSPs, followed by large $GABA_B$-mediated IPSPs in the cell (Fig. 1*C2*). In this case the fast EPSP/IPSPs generated spiky field potentials, followed by a slow positive wave caused by $GABA_B$ currents. This simple simulation therefore shows that, if excitatory and inhibitory cells generate high-frequency discharges in synchrony and if $GABA_B$ receptors are present, sufficient conditions are brought together to generate field potential waveforms consisting of interleaved spikes and waves.

The effect of various parameters on the morphology of simulated SW complexes was investigated in Figure 2*A*. When excitatory synapses discharged earlier than inhibitory synapses (2 and 5 msec latency), the spike component was enhanced. Spike and wave components also were influenced by synaptic conductances. AMPA and NMDA conductances affected primarily the negative peak of the spike component (Fig. 2*B, top trace*), whereas the positive peak was influenced mostly by $GABA_A$ conductances (Fig. 2*B, middle trace*). $GABA_B$ conductances had few effects on the spike component but mostly affected the wave (Fig. 2*B, bottom trace*).

Intact thalamic circuits can be forced into ~3 Hz oscillations because of $GABA_B$-mediated currents

To investigate how this type of field potentials can be generated by the thalamocortical system, we first turn to the behavior of thalamic circuits, and, more particularly, we turn to how they are controlled by the cortex. An important behavior of thalamic networks is their propensity to generate oscillations such as the 7–14 Hz spindle oscillations (Steriade et al., 1993; von Krosigk et al., 1993). Although these oscillations are generated in the thalamus, the neocortex has been shown to trigger them powerfully (Steriade et al., 1972; Roy et al., 1984; Contreras and Steriade, 1996), and the corticothalamic feedback has been shown to exert a decisive control over thalamic oscillations (Contreras et al., 1996).

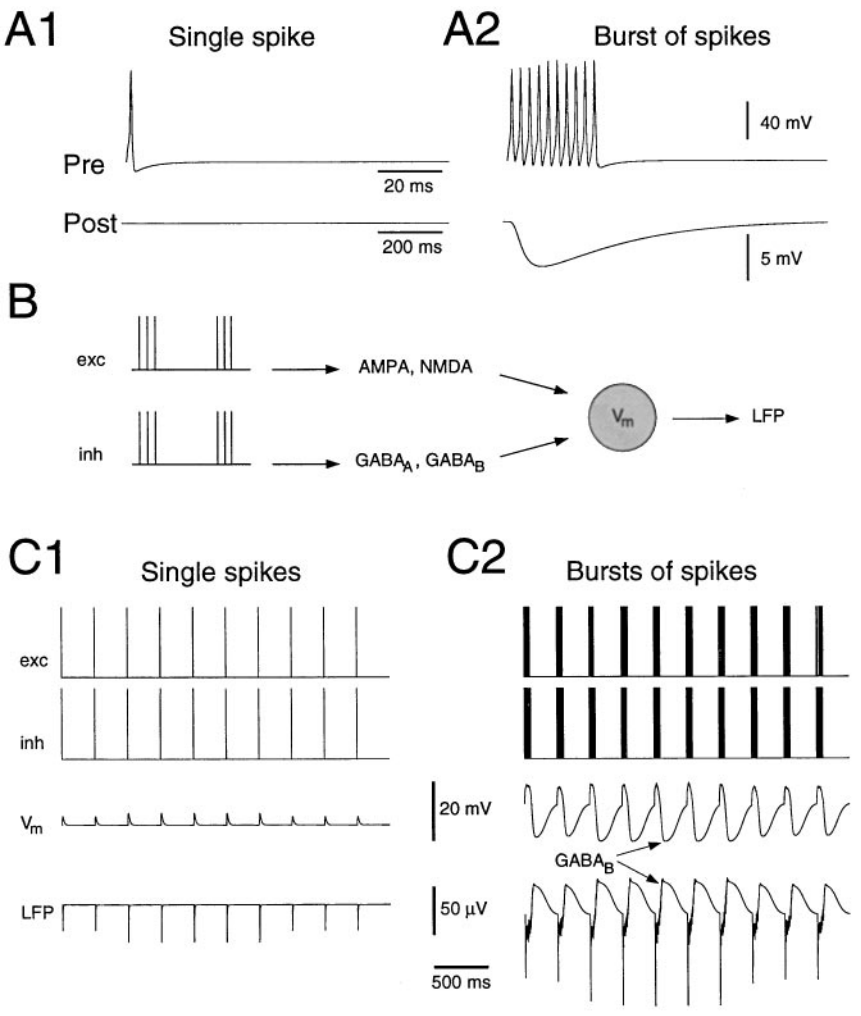

Figure 1. Simulation of spike and wave in field potentials, based on the properties of $GABA_B$ receptors. *A*, Nonlinear activation properties of $GABA_B$ receptors. If the binding of four G-proteins is needed to activate the K^+ channels associated with $GABA_B$ receptors, then $GABA_B$-mediated inhibitory responses are dependent on the number of presynaptic action potentials. *A1*, With a single presynaptic spike no $GABA_B$ response was detectable. *A2*, A burst of presynaptic spikes led to sufficient accumulation of G-proteins to generate the slow IPSP. *B*, Scheme for the model of local field potentials. Excitatory and inhibitory presynaptic trains of action potentials were generated to stimulate various postsynaptic receptor types (AMPA, NMDA, $GABA_A$, and $GABA_B$). One hundred synapses of each type were simulated, and the synaptic currents were integrated into a single compartment model and used to calculate the extracellular field potential at a distance of 5 μm from the simulated neuron. *C*, Field potentials generated by single spikes and bursts of spikes. With single spikes (*C1*) the mixed EPSP/IPSP sequence led to negative deflections in the field potentials. With bursts of spikes (*C2*) the fast spiky components alternate with slow positive deflections, similar to spike-and-wave patterns. These slow positive waves are attributable to the activation of $GABA_B$-mediated currents (*arrows*). Conductance values are 4, 1, 1.5, and 4 nS for individual AMPA, NMDA, $GABA_A$, and $GABA_B$ synapses, respectively.

In computational models, reproducing this cortical control required more powerful corticothalamic EPSPs on RE cells as compared with TC cells (Destexhe et al., 1998a). In these conditions the excitation of corticothalamic cells led to mixed EPSPs and IPSPs in TC cells in which the IPSP was dominant, consistent with experimental observations (Burke and Sefton, 1966; Deschênes and Hu, 1990). If cortical EPSPs and IPSPs from RE cells were of comparable conductance, cortical feedback could not evoke oscillations in the thalamic circuit because of shunting effects between EPSPs and IPSPs (Destexhe et al., 1998a). The most likely reason for these experimental and modeling evidences for "IPSP dominance" in TC cells is that RE cells are extremely sensitive to cortical EPSPs (Contreras et al., 1993), probably because of a powerful T-current in dendrites (Destexhe et al., 1996b). In addition, cortical synapses contact only the distal dendrites of TC cells (Liu et al., 1995) and probably are attenuated for this reason. Taken together, these data suggest that corticothalamic feedback operates mainly by eliciting bursts in RE cells, which in turn evoke powerful IPSPs on TC cells that in large part overwhelm the direct cortical EPSPs.

The effect of corticothalamic feedback on the thalamic circuit is depicted in Figure 3*A*: simulated cortical EPSPs evoked bursts in RE cells (Fig. 3*B, arrow*), which recruited TC cells via IPSPs, and triggered a ~10 Hz oscillation in the circuit. During the oscillation TC cells rebounded after $GABA_A$-mediated IPSPs once every two cycles, and RE cells discharged only a few spikes, evoking $GABA_A$-mediated IPSPs in TC cells with no significant $GABA_B$ currents (Fig. 3*B*). These features are typical of spindle oscillations (Steriade et al., 1993; von Krosigk et al., 1993).

Repetitive stimulation of the same thalamic circuit at 3 Hz with larger intensity (14 spikes every 333 msec) entrained the system into a different type of oscillatory behavior (Fig. 3*C*). All cell types were entrained to discharge in synchrony at ~3 Hz. On the other hand, repetitive stimulation at 3 Hz with low intensity produced spindle oscillations (Fig. 3*D*) similar to those in Figure 3*A*. Strong-intensity stimulation at 10 Hz led to quiescence in TC cells (Fig. 3*E*) because of sustained $GABA_B$ currents, similar to a previous analysis [Lytton et al. (1997), their Fig. 12].

These simulations indicate that strong corticothalamic feedback at 3 Hz can force thalamic circuits in a different type of oscillation. Cortical EPSPs force RE cells to fire large bursts (Fig. 3*C, arrows*), fulfilling the conditions needed to activate $GABA_B$ responses (see Fig. 1*A*). The consequence is that TC cells were "clamped" at hyperpolarized levels by $GABA_B$ IPSPs during ~300 msec before they could rebound. The nonlinear properties of $GABA_B$ responses are therefore responsible for the coexistence between two types of oscillations in the same circuit: mild corticothalamic feedback recruits the circuit in ~10 Hz spindle oscillations, whereas strong feedback at 3 Hz could force the intact circuit at the same frequency because of the nonlinear activation properties of intrathalamic $GABA_B$ responses.

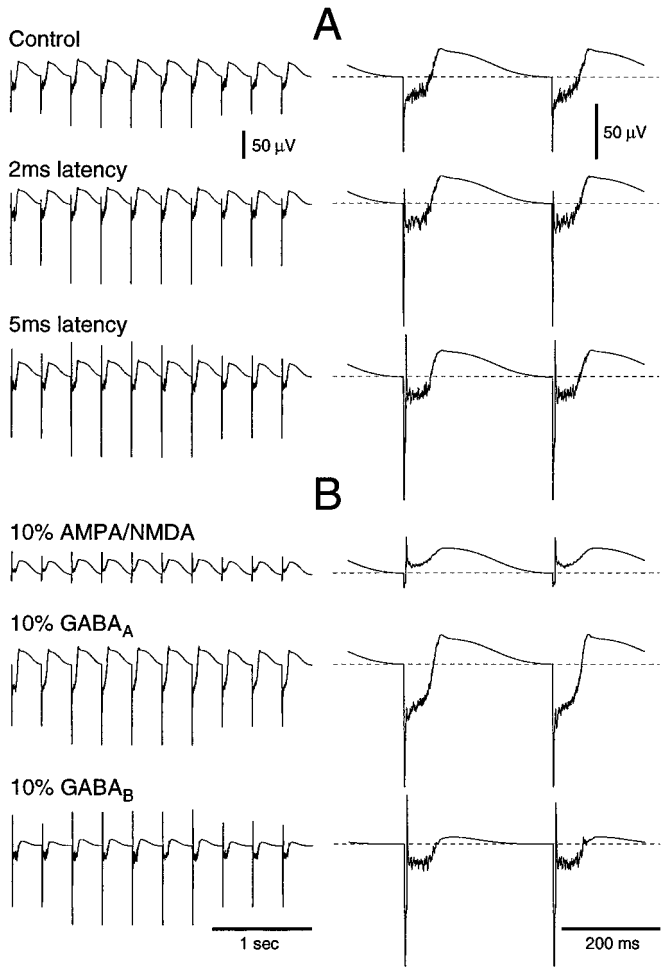

Figure 2. Factors determining the morphology of simulated spike-and-wave complexes. *A*, Effect of a latency between the firing of excitatory and inhibitory synapses. *Control*, Simulation is identical to Figure 1*C2*. If excitatory synapses discharged earlier than inhibitory synapses (2 and 5 msec latency), the spike component was enhanced. *B*, Effect of synaptic receptor types. The *5 msec latency* simulation from *A* was repeated here with different values for synaptic conductances. A 90% reduction of AMPA/NMDA conductances (*top trace*), $GABA_A$ conductances (*middle trace*), or $GABA_B$ conductances (*bottom trace*) affected the morphology of the SW patterns. The *right column* shows the last complexes at higher resolution.

Suppression of intrathalamic $GABA_A$-mediated inhibition does not generate spike and wave

The impact of this mechanism at the network level was explored using a thalamocortical network consisting in different layers of cortical and thalamic cells (see details in Materials and Methods). The network included thalamic TC and RE cells and a simplified representation of the deep layers of the cortex with pyramidal cells and interneurons (Fig. 4*A*). In control conditions (Fig. 4*B*) the network generated synchronized spindle oscillations with cellular discharges in phase between in all cell types, as observed experimentally (Contreras and Steriade, 1996). TC cells discharged on average once every two cycles after $GABA_A$-mediated IPSPs, whereas all other cell types discharged approximately at every cycle at ~10 Hz, consistent with the typical features of spindle oscillations observed intracellularly (Steriade et al., 1990; von Krosigk et al., 1993). The simulated field potentials displayed successive negative deflections at ~10 Hz (Fig. 4*B*; in agreement with the pattern of field potentials during spindle oscillations) (Steriade et al., 1990). Consistent with the analysis of Figure 1*C1*, this pattern of field potentials was generated by the limited discharge in PY cells, which fired approximately one spike per oscillation cycle.

When $GABA_A$ receptors were suppressed in thalamic cells in this model, with cortical inhibition intact, spindle oscillations were transformed into slower oscillation patterns at 3–5 Hz (Fig. 4*C*). In this case there was an increase in synchrony, as indicated by the TC cells that fired at every cycle of the oscillation. RE cells generated prolonged burst discharges, leading to $GABA_B$-mediated IPSPs in TC cells and, consequently, to a slow oscillation frequency. The field potentials consisted of successive negative deflections (Fig. 4*C, bottom*) similar to that of spindles. This pattern of field potentials was generated by PY cells that discharged approximately single spikes at each cycle of the oscillation (similar to Fig. 1*C1*). This simulation therefore suggests that removing intrathalamic $GABA_A$-mediated inhibition affects the oscillation frequency but does not generate SW, because pyramidal cells are still under the strict control of cortical fast inhibition. This is in agreement with *in vivo* injections of bicuculline into the thalamus, which reported slow oscillations with increased thalamic synchrony, but no SW patterns in the field potentials (Ralston and Ajmone-Marsan, 1956; Steriade and Contreras, 1998).

Suppression of intracortical $GABA_A$-mediated inhibition leads to spike and wave

On the other hand, the alteration of $GABA_A$ receptors in the cortex had a considerable impact in generating SW. When $GABA_A$-mediated inhibition was reduced in the cortex, with no change in thalamic inhibitory mechanisms, then spindle oscillations transformed into 2–3 Hz SW-like discharges (Fig. 5). With intracortical fast inhibition decreased by 50%, increased occurrences of prolonged high-frequency discharges were seen during spindle oscillations (Fig. 5*A*). In field potentials these events tended to generate large-amplitude negative deflections, followed by small-amplitude positive waves (Fig. 5*A, bottom*).

With totally suppressed $GABA_A$-mediated inhibition in the cortex, the network generated a slow oscillation at 2–3 Hz, with field potentials similar to SW (Fig. 5*B*). Field potentials displayed one or several negative/positive sharp deflections, followed by a slowly developing positive wave (Fig. 5*B, bottom*). During the spike all cells fired prolonged high-frequency discharges in synchrony, whereas the wave was coincident with neuronal silence in all cell types. This portrait is typical of experimental recordings of cortical and thalamic cells during SW patterns (Pollen, 1964; Steriade, 1974; Avoli et al., 1983; McLachlan et al., 1984; Buzsáki et al., 1990; Inoue et al., 1993). Some TC cells stayed hyperpolarized during the entire oscillation (second TC cell in Fig. 5*B*), as also was observed experimentally (Steriade and Contreras, 1995). A similar oscillation arose if $GABA_A$ receptors were suppressed in the entire network (data not shown).

These simulations thus indicate that spindles can be transformed into an oscillation with field potentials displaying SW and that this transformation can occur by the alteration of cortical inhibition with no change in the thalamus, in agreement with SW discharges obtained experimentally by diffuse application of diluted penicillin onto the cortex (Gloor et al., 1977). The mechanism of the ~3 Hz oscillation of this model depends on a thalamocortical loop in which both cortex and thalamus are necessary, but none of them generates the 3 Hz rhythmicity alone (see next section below).

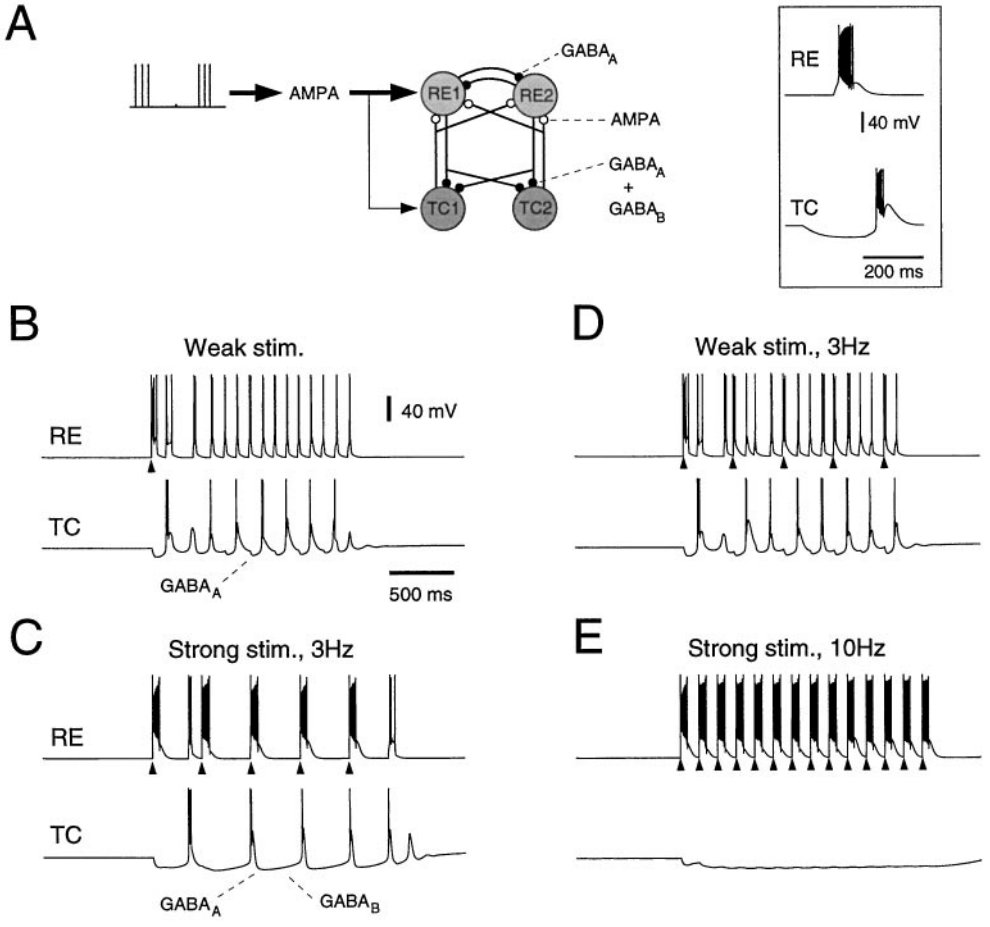

Figure 3. Corticothalamic feedback can force thalamic circuits into ~3 Hz oscillations because of the properties of $GABA_B$ receptors. *A*, Scheme of connectivity and receptor types in a circuit of thalamocortical (*TC*) and thalamic reticular (*RE*) neurons. Corticothalamic feedback was simulated through AMPA-mediated synaptic inputs (shown on the *left* of the connectivity diagram; total conductance was 1.2 μS to RE cells and 0.01 μS to TC cells). The *inset* shows simulated burst responses of TC and RE cells after current injection (pulse of 0.3 nA during 10 msec for RE and −0.1 nA during 200 msec for TC). *B*, A single stimulation of corticothalamic feedback (*arrowhead*) entrained the circuit into a 10 Hz mode similar to that for spindle oscillations. *C*, With a strong-intensity stimulation at 3 Hz (*arrowheads*; 14 spikes per stimulus), RE cells were recruited into large bursts, which evoked IPSPs onto TC cells dominated by $GABA_B$-mediated inhibition. In this case the circuit could be entrained into a different oscillatory mode, with all cells firing in synchrony. *D*, Weak stimulation at 3 Hz (*arrowheads*) entrained the circuit into spindle oscillations (identical intensity as in *B*). *E*, Strong stimulation at 10 Hz (*arrowheads*) led to quiescent TC cells because of sustained $GABA_B$ current (identical intensity as in *C*).

The progressive transformation between spindles and SW oscillations in the model is shown in Figure 6. With intact cortical inhibition the discharge of cells in the network was limited to a few spikes. Consequently, IPSPs in PY cells were almost exclusively $GABA_A$-mediated, leading to field potentials consisting of negative deflections only (Fig. 6, 100%). With the intracortical inhibition partially reduced, there was an increased tendency of producing prolonged discharges and an increased contribution of $GABA_B$ IPSPs in PY cells, leading to small positive waves in field potentials (Fig. 6, 50%). With a further reduction of intracortical $GABA_A$-mediated inhibition, the system showed fully developed SW complexes in field potentials, with oscillation frequencies within the 2–3 Hz range (Fig. 6, from 25 to 0%). The frequency of SW oscillations was approximately proportional to the amount of fast inhibition still present in the cortex. The occurrence of a positive spike also was correlated with intracortical fast inhibition (Fig. 6), in agreement with the effect of $GABA_A$ conductances in Figure 2*B*.

The waxing and waning appearance of spindles (Fig. 6, 100%) was attributable here to intrathalamic mechanisms. A calcium-dependent upregulation of I_h in TC cells was included here, similar to previous models (Destexhe et al., 1993, 1996a). Such regulation was demonstrated recently in thalamic slices (Lüthi and McCormick, 1998). This mechanism was responsible for the waxing and waning of oscillations in model thalamic and thalamocortical networks (Destexhe et al., 1996a, 1998a). It interesting to note that SW oscillations also may follow a similar waxing and waning envelope (Fig. 6, 25%), which was attributable here to the same intrathalamic mechanisms as spindles. The model therefore suggests that the calcium-dependent upregulation of I_h in TC cells is responsible for the temporal modulation of SW oscillations and may lead to bursts of several cycles of SW oscillations, interleaved with long periods of silence (~20 sec), as are observed experimentally in sleep spindles and SW epilepsy, thus stressing further the resemblance between the two types of oscillation.

A thalamocortical loop mechanism for spike-and-wave oscillations

The thalamocortical mechanism leading to SW oscillations in this model is illustrated and compared with spindles in Figure 7. During spindles the oscillation is generated by intrathalamic interactions (TC–RE loop in Fig. 7*A*). Oscillations can also be generated by a thalamocortical loop (TC–Cx–RE loop in Fig. 7*A*), as suggested previously (Destexhe et al., 1998a). The combined action of intrathalamic and thalamocortical loops provides a moderate excitation of RE cells, which evokes $GABA_A$-mediated IPSPs in TC cells and sets the frequency to ~10 Hz. During SW oscillations (Fig. 7*B*) an increased cortical excitability provides a corticothalamic feedback that is strong enough to force prolonged burst discharges in RE cells, which in turn evoke IPSPs in TC cells dominated by the $GABA_B$ component. In this case the prolonged inhibition sets the frequency to ~3 Hz. The oscillation is generated by a thalamocortical loop (TC–Cx–RE loop in Fig. 7*B*) in which the thalamus is intact. Therefore, if the cortex is inactivated during SW, this model predicts that the thalamus

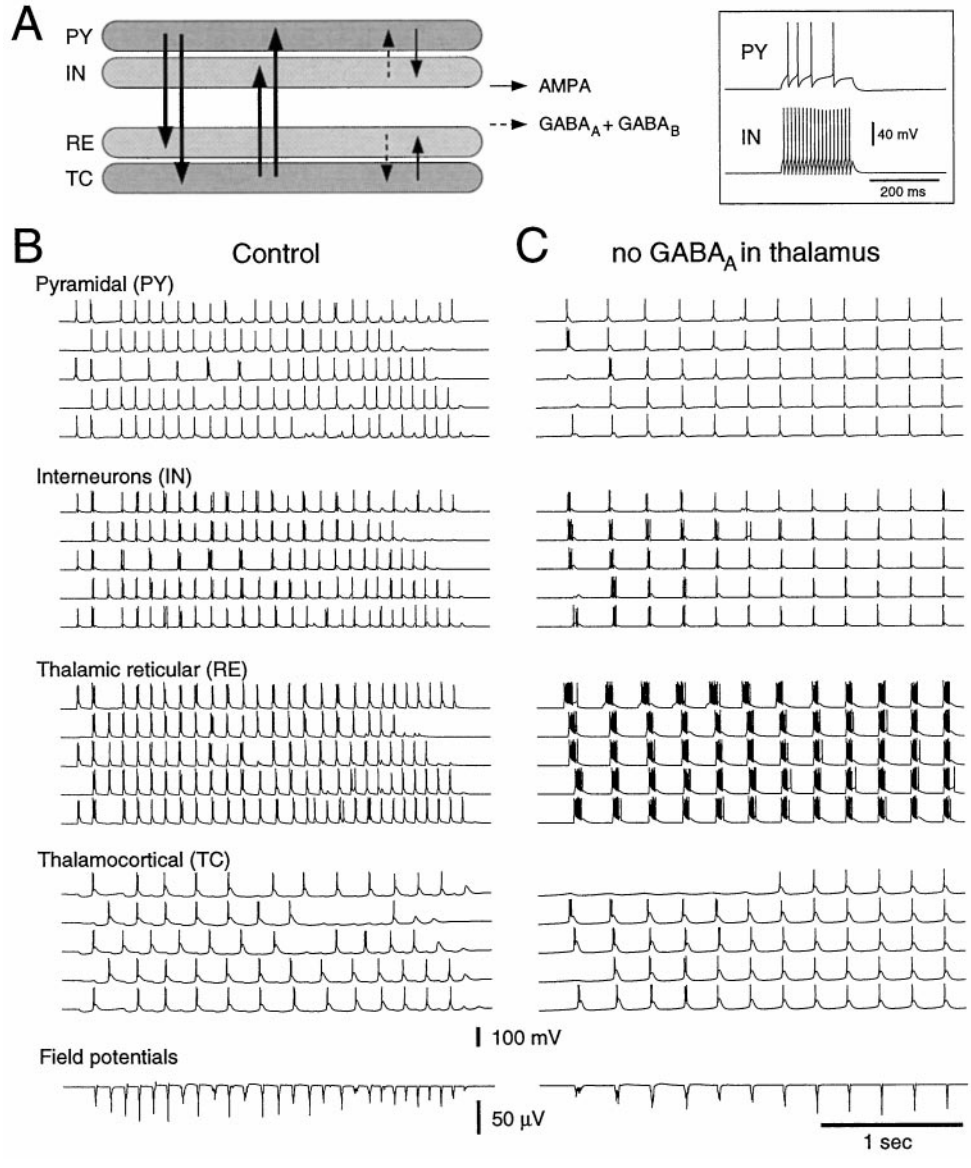

Figure 4. Transformation of spindle oscillations into ~4 Hz oscillations by blocking thalamic inhibition in thalamocortical networks. *A*, Scheme of the connectivity among different cell types: 100 cells of each type were simulated, including thalamocortical (*TC*) and thalamic reticular (*RE*) cells, cortical pyramidal cells (*PY*), and interneurons (*IN*). The connectivity is shown by *continuous arrows*, representing AMPA-mediated excitation, and *dashed arrows*, representing mixed $GABA_A$ and $GABA_B$ inhibition. In addition, PY cells were interconnected by using AMPA receptors, and RE cells were interconnected by using $GABA_A$ receptors. The *inset* shows the repetitive firing properties of PY and IN cells that follow depolarizing current injection (0.75 nA during 200 msec; −70 mV rest). *B*, Spindle oscillations in the thalamocortical network in control conditions. Five cells of each type, equally spaced in the network, are shown (0.5 msec time resolution). The field potentials, consisting of successive negative deflections at ~10 Hz, are shown at the *bottom*. *C*, Oscillations after the suppression of $GABA_A$-mediated inhibition in thalamic cells with cortical inhibition intact (all $GABA_A$ conductances postsynaptic to RE cells were suppressed). The network generated synchronized oscillations at ~4 Hz, with thalamic cells displaying prolonged discharges. PY cells showed discharge patterns similar to those of spindles but at a slower frequency; so did the field potentials (*bottom*).

should resume generating spindle oscillations, as observed experimentally in cats treated with penicillin (Gloor et al., 1979).

The relation between cellular events and field potentials in this model of SW is shown in Figure 8. The pattern displayed by the network is similar to Figure 1*C2*: high-frequency discharges generated spike components in the field potentials, whereas wave components were generated by $GABA_B$ IPSPs in PY cells because of the prolonged firing of cortical interneurons. The hyperpolarization of PY cells during the wave also contained a significant contribution from the voltage-dependent K^+ current I_M (data not shown), maximally activated because of the prolonged discharge of PY cells during the spike. The wave component is therefore attributable in this model to two types of K^+ currents, intrinsic and $GABA_B$-mediated. The relative contribution of each current to the wave depends on its respective conductance values.

During the spike component the discharges were not perfectly in phase. As indicated in Figure 8*B*, there was a significant phase advance of TC cells, as observed experimentally (Inoue et al., 1993). This phase advance was responsible for the initial negative spike in the field potentials, which coincided with the first spike in the TC cells (Fig. 8*B, dashed line*). This feature implements the precedence of EPSPs over IPSPs in the PY cell to generate SW complexes, as evidenced above (see Fig. 2*A*). The simulations therefore suggest that the initial spike of SW complexes is attributable to thalamic EPSPs that precede other synaptic events in PY cells.

Determinants of spike-and-wave oscillations

The critical factors involved in the genesis of SW oscillations in the thalamocortical model were characterized by investigating the range of synaptic conductances giving rise to SW for each type of connection in the absence of intracortical $GABA_A$-mediated inhibition (Table 1). It must be noted that this model considered greatly simplified single-compartment models of thalamic and cortical neurons, with minimal sets of intrinsic currents, no dendrites (and therefore no dendritic currents and no dendritic synapses), and simplified models of intrinsic and synaptic currents. The conductance values therefore cannot match quantitatively the physiological values and must be interpreted qualitatively.

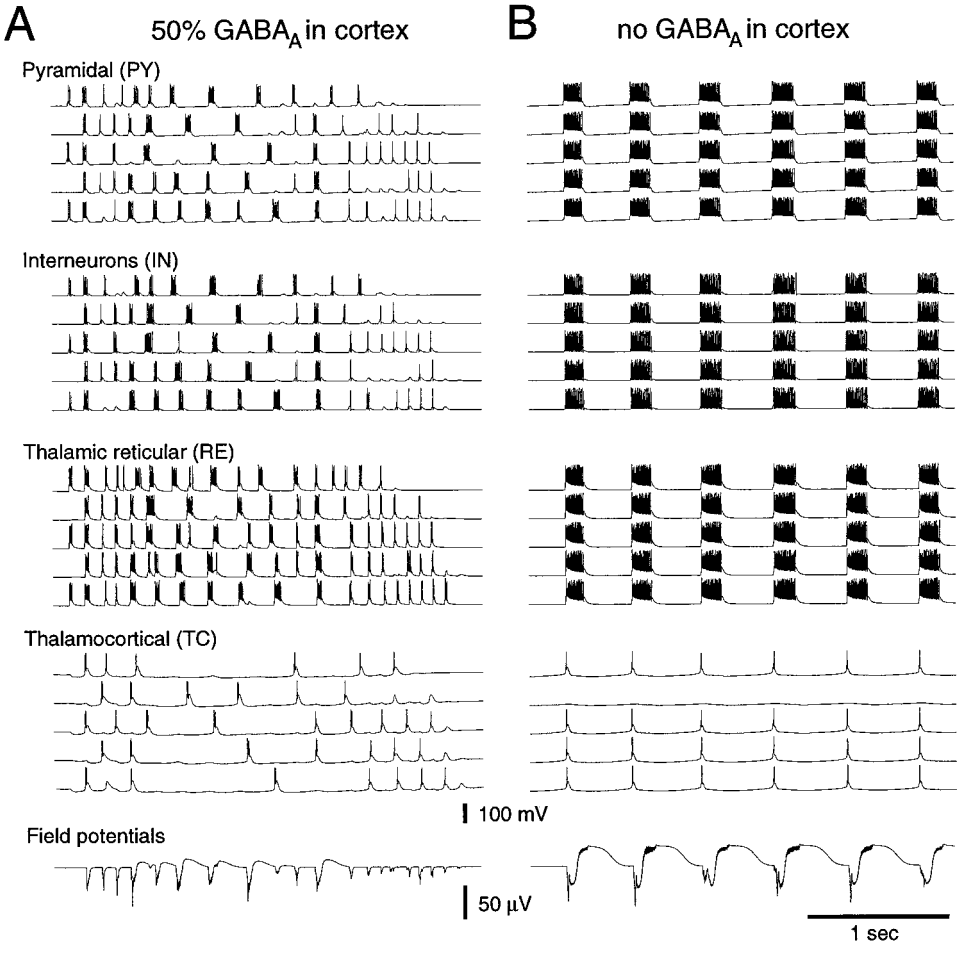

Figure 5. Transformation of spindle oscillations into ~3 Hz oscillations with spike-and-wave field potentials by reducing cortical inhibition. Shown is a similar arrangement of traces as in Figure 4, *B* and *C*. *A*, Oscillations with a 50% decrease of $GABA_A$-mediated inhibition in cortical cells (0.075 μS, IN→PY). Stronger burst discharges appeared within spindle oscillations, leading to large-amplitude negative spikes, followed by small positive waves in the field potentials (*bottom*). *B*, Oscillations after suppression of $GABA_A$-mediated inhibition in cortical cells. All cells displayed prolonged discharges in phase, separated by long periods of silences, at a frequency of ~2 Hz. $GABA_B$ currents were activated maximally in TC and PY cells during the periods of silence. Field potentials (*bottom*) displayed spike-and-wave complexes. Thalamic inhibition was intact in *A* and *B*.

Table 1 shows the optimal values of the conductance that were used and, for each connection, the range of values leading to SW oscillations. The minimal frequency of SW bursts when each parameter was varied within 50–200% of the optimal value is indicated in the last two columns of Table 1. The synaptic conductances that were influential on SW were PY→PY, PY→IN, IN→PY, RE→RE, RE→TC ($GABA_B$), PY→RE, and a weak effect for RE→TC ($GABA_A$). TC→RE, TC→PY, TC→IN, and PY→TC had minimal effect. As expected, the recurrent excitation between pyramidal cells (PY→PY) and the excitation of interneurons (PY→IN), as well as the inhibitory feedback on PY cells (IN→PY), are effective on SW because these conductance determine the excitability of the cortical network. Less expected was the role of cortical excitatory feedback on RE cells (PY→RE), intra-RE inhibition (RE→RE), and the $GABA_B$ inhibition from RE onto TC cells (RE→TC). These factors are examined in more detail below.

A first influential factor was the intra-RE GABAergic connections. Figure 9*A* shows the transition curve from SW oscillations to spindle waves as a function of intracortical $GABA_A$ inhibition, similar to Figure 6. Reinforcing intra-RE $GABA_A$ inhibition significantly reduced SW in favor of the spindles (Fig. 9*A*, compare *open triangles* with *filled circles*), whereas decreasing this inhibition had the opposite effect (Fig. 9*A*, *open squares*). In the model, reinforcing intra-RE $GABA_A$-mediated inhibition diminished the tendency of RE cells to produce bursts of action potentials, therefore diminishing $GABA_B$-mediated IPSPs in TC cells and reducing the tendency to generate SW oscillations. This behavior is consistent with the presumed role of the anti-absence drug clonazepam, which may reduce the tendency of the network to produce SW by specifically acting on $GABA_A$ receptors in the thalamic RE nucleus (Huguenard and Prince, 1994a; Gibbs et al., 1996; Hosford et al., 1997).

A second factor that was particularly effective on SW was the corticothalamic feedback on RE cells. Reducing the AMPA conductance of cortical EPSPs on RE cells significantly diminished SW in favor of the spindles (Fig. 9*B*, compare *open triangles* with *filled circles*), and increasing this conductance had the opposite effect. The model therefore indicates that diminishing the impact of corticothalamic EPSPs on RE cells is a potential factor in reducing the threshold for SW in the network.

The need for larger conductances of cortical EPSPs in RE cells versus TC cells also is evidenced for SW oscillations, similar to a previous suggestion in the context of spindle oscillations (Destexhe et al., 1998a). SW oscillations coexisting with spindles required at least four times larger AMPA conductances on RE cells (0.4 μS for PY→RE and 0.1 μS of PY→TC in Table 1). This is consistent with the anatomical observation that cortical synapses contact only the distal dendrites of TC cells (Liu et al., 1995), leading to attenuated cortical EPSPs.

An additional influential factor, not included in Table 1, was the T-current conductance in RE cells. Reducing the T-current of RE cells significantly reduced SW in favor of the spindles (Fig. 9*C*, compare *open triangles* with *filled circles*), whereas reinforcing this current had the opposite effect (Fig. 9*C, open squares*). Reducing T-current amplitude therefore diminishes the tendency of the

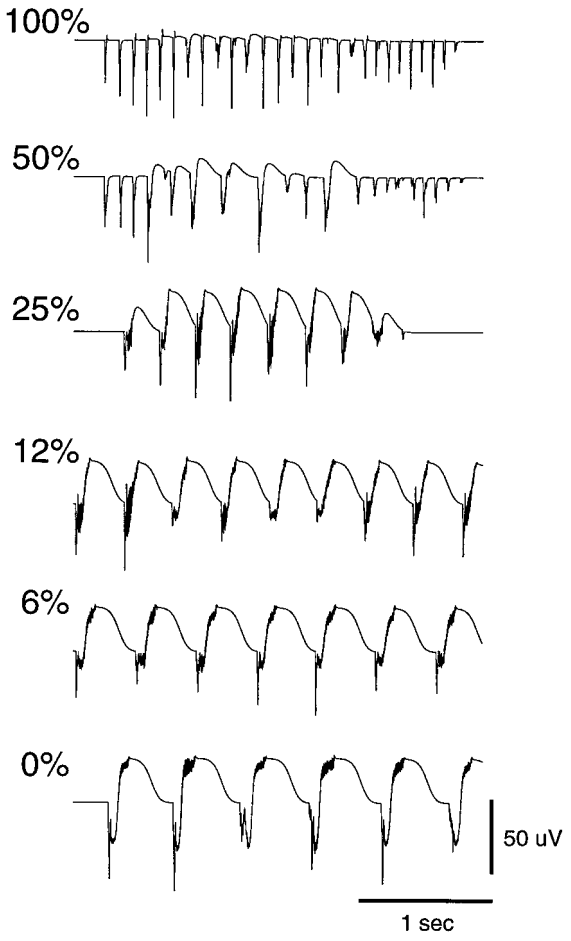

Figure 6. Gradual transformation of spindles to spike-and-wave complexes. The field potentials obtained for different simulations similar to Figure 5 are shown from *top* to *bottom*. The different simulations correspond to identical conditions, except that intracortical $GABA_A$-mediated inhibition (IN→PY) was reduced, with total conductance values of 0.15 μS (100%), 0.075 μS (50%), 0.0375 μS (25%), 0.018 μS (12%), and 0.009 μS (6%). *100%* corresponded to a spindle sequence (same simulation as in Fig. 4*B*) and *0%* to fully developed SW complexes when the intracortical $GABA_A$ inhibition was suppressed (same simulation as in Fig. 5*B*); intrathalamic inhibition was intact in all cases.

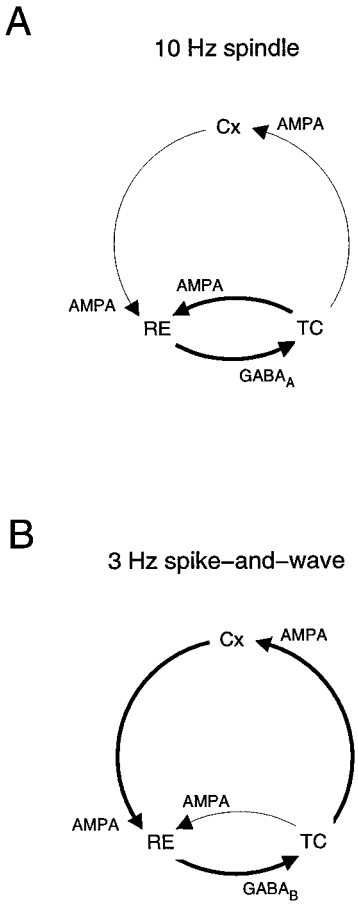

Figure 7. Thalamocortical loop mechanism for spike and wave. Simplified diagrams represent the major steps involved in generating oscillations (*Cx*, cortex). *A*, Spindle oscillations resulting from a mutual recruitment of thalamic TC and RE cells (*thick lines*) in which TC cells rebound after fast $GABA_A$-mediated IPSPs, setting the frequency to ~10 Hz. Here, the oscillation is generated in the thalamus and is reinforced by the thalamocortical loop (*thin lines*). *B*, Proposed mechanism for spike and wave. In this case the corticothalamic feedback is much stronger because of increased cortical excitability, forcing thalamic cells to display prolonged burst discharges, which evoke $GABA_B$-mediated IPSPs in TC cells. This prolonged inhibition prevents cells from firing during ~300 msec and sets the frequency to ~3 Hz.

network to produce SW, similar to reinforcing GABAergic inhibition in the RE nucleus. This effect is consistent with the experimental finding that the T-current is increased selectively in RE cells in a rat model of absence epilepsy (Tsakiridou et al., 1995).

On the other hand, reducing the T-current conductance in TC cells had only a weak effect on SW threshold (data not shown), but T-current reduction >40% in TC cells led to the suppression of oscillatory behavior. This was consistent with the effect of the anti-absence drug ethosuximide in reducing the total T-current conductance in TC cells (Coulter et al., 1989).

As predicted from the mechanism of Figure 7*B*, the frequency of SW essentially was determined by $GABA_B$-mediated IPSPs on TC cells (Fig. 9*D, filled circles*). Changing the decay of intrathalamic $GABA_B$ currents (parameter K_4) affected only the frequency, with minimal changes in the bursting patterns of the different cell types (data not shown). This effect was attributable to the fact that, in this model, the duration of the wave is determined essentially by $GABA_B$ IPSPs in TC cells, longer IPSPs leading to slower SW by further delaying the rebound of TC cells. The frequency varied from 1 to 5 Hz for decay values of 50–250% of the control value, suggesting that the different frequency of SW bursts in different experimental models may be attributable to differences in the kinetics of $GABA_B$-mediated inhibition in TC cells.

The T-current amplitude in TC cells also affected the SW frequency (Fig. 9*D, open squares*). Stronger T-current conductances led to earlier rebound and faster frequencies. By contrast, the T-current amplitude in RE cells had minimal effect on SW frequency (Fig. 9*C, open triangles*). Consistent with the mechanism depicted in Figure 7*B*, the frequency of SW was mostly attributable to intrathalamic mechanisms, whereas the threshold for SW was dependent on the different elements involved in the thalamus–cortex–thalamus loop.

DISCUSSION

This paper proposed a thalamocortical loop mechanism for the genesis of spike-and-wave oscillations. This mechanism, its simi-

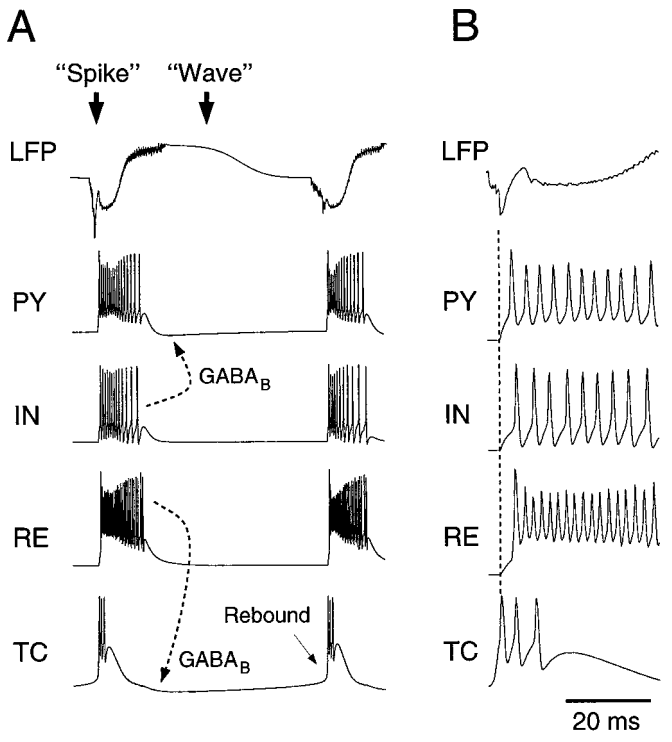

Figure 8. Phase relations during simulated spike-and-wave discharges. *A*, Local field potentials (*LFP*) and representative cells of each type during SW oscillations. *Spike*, All cells displayed prolonged discharges in synchrony, leading to spiky field potentials. *Wave*, The prolonged discharge of *RE* and *IN* neurons evoked maximal $GABA_B$-mediated IPSPs in *TC* and *PY* cells, respectively (*dashed arrows*), stopping the firing of all neuron types during a period of 300–500 msec and generating a slow positive wave in the field potentials. The next cycle restarted because of the rebound of *TC* cells after the $GABA_B$ IPSP (*arrow*). *B*, Phase relationships in the thalamocortical model. *TC* cells discharged first, followed by *PY*, *RE*, and *IN* cells. The initial negative peak in the field potentials coincided with the first spike in *TC* cells before the *PY* cells started firing and was generated by thalamic EPSPs in *PY* cells.

larities and differences with experimental SW, plus predictions to test its validity are discussed successively.

A $GABA_B$-based mechanism for spike and wave

The cellular mechanism proposed here is based on the following properties:

(1) Because of the characteristics of $GABA_B$-mediated responses, simulated field potentials can display SW waveforms if cortical pyramidal cells and interneurons generate prolonged discharges in synchrony, without the need of any other assumption about intrinsic cellular or circuit mechanisms.

(2) Also because of the characteristics of $GABA_B$-mediated inhibition, model thalamic circuits can be forced into ~3 Hz oscillations. It is known from slice experiments that thalamic circuits naturally oscillate at ~10 Hz but display ~3 Hz oscillations in the presence of $GABA_A$-receptor agonists (von Krosigk et al., 1993). The present model suggests that a similar oscillation can be forced in *intact* thalamic circuits if corticothalamic feedback EPSPs are strong enough.

(3) Generalized ~3 Hz oscillations can be generated through thalamocortical loops. If because of an increase of cortical excitability the thalamic-projecting cortical cells generate exceedingly strong discharges, then the ensuing corticothalamic feedback EPSPs may become strong enough to force the thalamus in the 3 Hz mode. The ~3 Hz oscillations then invade the entire network through thalamocortical loops. The ~3 Hz frequency depends on intrathalamic $GABA_B$-mediated inhibition.

(4) This ~3 Hz oscillation generates SW field potentials. During the spike the thalamic and cortical cells produce prolonged discharges in synchrony, whereas the wave is generated by a mixture of voltage-dependent and $GABA_B$-mediated K^+ currents.

Similarities with experimental models of spike and wave

This thalamocortical loop model is consistent with a number of experimental results on SW epilepsy: (1) thalamic and cortical neurons discharge in synchrony during the spike, whereas the wave is characterized by neuronal silence (Pollen, 1964; Steriade, 1974; Avoli et al., 1983; McLachlan et al., 1984; Buzsáki et al., 1990; Inoue et al., 1993), similar to the data in Figures 4*E* and 8*A*; (2) TC cell firing precedes that of other cell types, followed by cortical cells and RE cells (Inoue et al., 1993), similar to the phase relations of the present model (see Fig. 8*B*); (3) SW patterns disappear after the removal of either the cortex (Avoli and Gloor, 1982) or the thalamus (Pellegrini et al., 1979; Vergnes and Marescaux, 1992), as also predicted by the present mechanism; (4) antagonizing thalamic $GABA_B$ receptors suppresses SW discharges (Liu et al., 1992), consistent with this model; (5) spindle oscillations can be transformed gradually into SW discharges (Kostopoulos et al., 1981a,b), as described in Figure 6.

The present mechanism also emphasizes a critical role for the RE nucleus. Reinforcing $GABA_A$-mediated inhibition in the RE nucleus will antagonize the genesis of large burst discharges in RE cells by corticothalamic EPSPs, antagonizing the genesis of $GABA_B$-mediated IPSPs in TC cells and therefore antagonizing SW. This property is consistent with the diminished frequency of seizures that is observed after the reinforcement of $GABA_A$ receptors in the RE nucleus (Liu et al., 1991). It is also consistent with the action of the anti-absence drug clonazepam, which seems to act preferentially by enhancing $GABA_A$ responses in the RE nucleus (Hosford et al., 1997), leading to diminished $GABA_B$-mediated IPSPs in TC cells (Huguenard and Prince, 1994a; Gibbs et al., 1996).

The fact that injections of $GABA_A$ antagonists in the thalamus with intact cortex failed to generate SW (Ralston and Ajmone-Marsan, 1956; Gloor et al., 1977; Steriade and Contreras, 1998) also was considered. In the model, suppressing thalamic $GABA_A$ receptors led to "slow spindles" at ~4 Hz, very different from SW oscillations (see Fig. 4*C*). In this case the discharge of PY cells was extremely brief, because cortical $GABA_A$-mediated inhibition was preserved and no $GABA_B$ IPSPs could be evoked. This result is consistent with the powerful control exerted on pyramidal cells by intracortical $GABA_A$-mediated inhibition, as shown by intracellular recordings and modeling (Contreras et al., 1997).

Differences with experimental models of spike and wave

On the other hand, a number of experimental observations are not consistent with the mechanism presented here. First, an apparent intact cortical inhibition was reported in cats treated with penicillin (Kostopoulos et al., 1983). However, this study did not distinguish between $GABA_A$ and $GABA_B$-mediated inhibition. In the present model, even when $GABA_A$ was antagonized, IPSPs remained approximately the same size because cortical interneurons fired stronger discharges (see Fig. 4*D,E*) and led to stronger $GABA_B$ currents. There was a compensation effect between $GABA_A$- and

Table 1. Range of values for synaptic conductances and their effect on spike-and-wave oscillations

Receptor type	Location	Optimal value	SW range	SW frequency (50%) in Hz	SW frequency (200%) in Hz
AMPA	PY→PY	0.6 μS	0.3–0.9 μS	3.0	—
AMPA	PY→IN	0.2 μS	0.06–2 μS	1.3	1.9
$GABA_B$	IN→PY	0.03 μS	0.02–5 μS*	1.3	2.0
AMPA	TC→RE	0.2 μS	0–5 μS*	1.7	1.7
$GABA_A$	RE→RE	0.2 μS	0–1.2 μS	1.4	2.5
$GABA_A$	RE→TC	0.02 μS	0–1 μS	1.7	1.8
$GABA_B$	RE→TC	0.04 μS	0.01–5 μS*	2.1	1.3
AMPA	TC→PY	1.2 μS	0.15–5 μS*	1.7	1.7
AMPA	TC→IN	0.4 μS	0–5 μS*	1.7	1.7
AMPA	PY→RE	1.2 μS	0.4–5 μS*	2.2	1.5
AMPA	PY→TC	0.01 μS	0–0.1 μS	1.7	1.7

Conductance values represent the sum of all individual synaptic conductances of the same type converging to a given cell. The range of conductance values giving rise to SW oscillations is indicated in the fourth column (*no value >5 μS was tested, because sodium spike inactivation may occur for too high conductance values). The minimal oscillation frequency is indicated in the last two columns when each respective conductance was set to 50 and 200% of the optimal value; a value equal to control (1.7 Hz) indicates that this parameter had no detectable influence on SW. All simulations were run by using the thalamocortical network model with suppressed $GABA_A$-mediated inhibition in cortical cells (same conditions as in Fig. 5*B*).

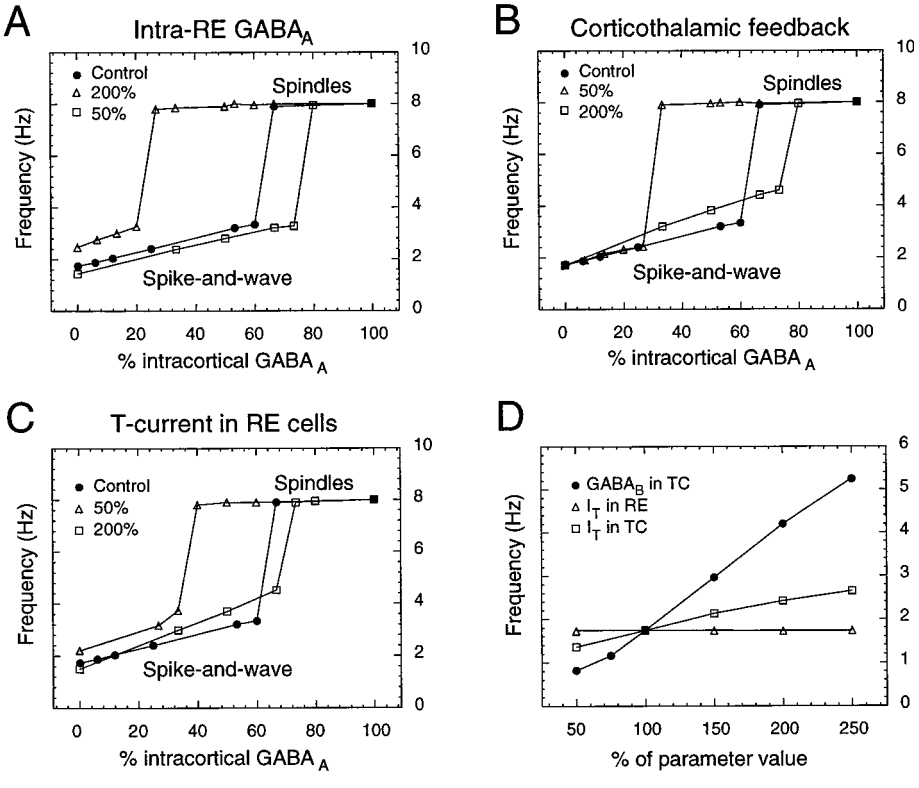

Figure 9. Determinants of spike-and-wave oscillations. *A*, Effect of $GABA_A$-mediated inhibition between RE cells. The lowest frequency of SW complexes is represented as a function of the amount of $GABA_A$ inhibition in cortex (simulations similar to Fig. 6). In control (*filled circles*) the frequency of SW increased steadily up to 60% of cortical $GABA_A$; then a transition occurred to spindle oscillations (lowest frequency of ~8 Hz). With twice smaller intra-RE $GABA_A$ conductances (*open squares*) this transition occurred at ~75% cortical $GABA_A$. When intra-RE $GABA_A$ conductances were doubled, the domain of SW was significantly smaller, with a transition occurring at ~20% of cortical $GABA_A$ (*open triangles*). *B*, Effect of corticothalamic feedback on RE cells. With diminished AMPA conductance in PY→RE synapses (50% of control value), the domain of SW was reduced significantly (*open triangles*), whereas reinforced cortical EPSPs had the opposite effect (*open squares*). *Filled circles*, Same control as in *A*. *C*, Effect of the T-current conductance in RE cells. With reinforced T-current (200% of control value) the transition occurred at ~75% of cortical $GABA_A$ (*open squares*), whereas with diminished T-current (50% of control value) the domain of SW was reduced significantly (*open triangles*). *Filled circles*, Same control as in *A*. *D*, Determinants of SW frequency. The frequency of SW bursts in the simulation of Figure 5*B* was represented when several parameters were varied. These parameters are represented as the percentage of their control value (100% = control). The parameters represented are the decay of intrathalamic $GABA_B$ currents (*filled circles*), the T-current conductance in TC (*open squares*), and RE cells (*open triangles*).

$GABA_B$-mediated IPSPs (data not shown), which may lead to the misleading observation that inhibition is preserved.

Second, some $GABA_A$ agonists, like barbiturates, may increase the frequency of seizures (Vergnes et al., 1984), possibly via interactions with $GABA_A$ receptors in TC cells (Hosford et al., 1997). A similar effect was seen in the model (Table 1, $GABA_A$ RE→TC), but this effect was weak. To be simulated more precisely, this type of data would require modeling the variants of $GABA_A$ receptor types in different cells and addressing how the threshold for SW discharges is affected by various types of GABAergic conductances. These points should be considered in future models.

Third, the present model investigated only a thalamocortical loop scenario for the genesis of SW oscillations, but other mechanisms are possible. Although most experimental data are in favor of a mechanism involving both thalamus and cortex (see introductory remarks), numerous experimental evidence also points to a possible intracortical mechanism for SW. Experiments revealed SW in isolated cortex or athalamic preparations in cats (Marcus and Watson, 1966; Pellegrini et al., 1979; Steriade and Contreras, 1998). However, this type of paroxysmal oscillation had a different morphology and was slower in frequency compared with the typical "thalamocortical" SW (1–2.5 vs 3.5–5 Hz; Pellegrini et al., 1979). By contrast, intracortical SW was not

observed in athalamic rats (Vergnes and Marescaux, 1992). Because no intracellular recordings were made during the presumed SW in cat isolated cortex, it is not clear if this oscillation represents the same SW paroxysm as in the intact thalamocortical system. Nevertheless, the cortex is known to display intrinsic oscillations generated by bursting neurons (Silva et al., 1991) and also contains rebound-bursting pyramidal cells in some cortical areas (de la Pena and Geijo-Barrientos, 1996). It may be that these properties are sufficient to sustain a form of purely cortical SW, via a sequence of $GABA_B$ IPSPs and rebound, similar to the mechanism analyzed here. When more precise experimental data become available, such as intracellular recordings, possible intracortical mechanisms for SW should be investigated by future models.

Predictions

Several predictions are generated by this model. First, the wave component of SW was generated by massive K^+ currents, mostly because of $GABA_B$ receptor activation. This could be observable by performing intracellular recordings during SW while blocking $GABA_B$ responses. At the network level the injection of $GABA_B$ antagonists or K^+ currents blockers on the cortex should lead to significant alteration of the wave component in field potentials. One must, however, bear in mind that other mechanisms not taken into account here also may participate to the wave component, such as the activation of Ca^{2+} spikes and Ca^{2+}-dependent K^+ currents, possibly in dendrites (Traub and Miles, 1991).

A second prediction is that intact thalamic circuits can be forced into a ~3 Hz oscillation by strong stimulation of corticothalamic feedback fibers. This experiment could be performed in slices or in decorticated animals by stimulating the internal capsule. The intensity should be high enough to force large bursts in RE cells, evoking $GABA_B$ IPSPs in TC cells and delaying their rebound by ~300 msec. Two stimulation patterns are possible: either the stimulation period should match the delay to rebound, or the stimulation could be triggered by the multiunit discharge of TC cells. In the latter case the model predicts a switch from ~10 Hz oscillations to ~3 Hz when the stimulation intensity is increased.

Finally, the model predicts a critical role for the dependence of $GABA_B$ IPSPs on the number of presynaptic spikes. This effect was simulated by assuming that the binding of four G-proteins is required to activate the K^+ channels underlying $GABA_B$ responses (Destexhe and Sejnowski, 1995). In the thalamocortical model the dependence on the number of spikes is critical for generating the ~3 Hz oscillations as well as the spike-and-wave waveform in field potentials. Dual intracellular recordings between cortical inhibitory interneurons and their targets should shed light into this question in the near future (A.M. Thomson and A. Destexhe, unpublished data).

In conclusion, this paper suggests a thalamocortical loop mechanism for spike and wave, based on the intrinsic and synaptic properties of thalamic and cortical cells, the characteristics of which are consistent with several experimental models of SW as well as with thalamic slice experiments. The key biophysical components of this mechanism are the activation properties of $GABA_B$ receptors, combined with the complex intrinsic firing properties of thalamic cells. The model also emphasizes a major role for corticothalamic feedback in triggering powerful bursts in RE cells, by which the cortex can force the thalamus to generate oscillations at ~3 Hz by activating intrathalamic $GABA_B$-mediated inhibition. Because thalamic RE cells may generate bursts through dendritic T-currents (Destexhe et al., 1996b), their sensitivity to corticothalamic feedback EPSPs therefore may be maximal (Contreras et al., 1993), leading to the prediction that this structure should be a major target for a possible suppression of seizures.

REFERENCES

Avoli M, Gloor P (1981) The effect of transient functional depression of the thalamus on spindles and bilateral synchronous epileptic discharges of feline generalized penicillin epilepsy. Epilepsia 22:443–452.

Avoli M, Gloor P (1982) Role of the thalamus in generalized penicillin epilepsy: observations on decorticated cats. Exp Neurol 77:386–402.

Avoli M, Gloor P, Kostopoulos G, Gotman J (1983) An analysis of penicillin-induced generalized spike and wave discharges using simultaneous recordings of cortical and thalamic single neurons. J Neurophysiol 50:819–837.

Burke W, Sefton AJ (1966) Inhibitory mechanisms in lateral geniculate nucleus of rat. J Physiol (Lond) 187:231–246.

Buzsáki G, Smith A, Berger S, Fisher LJ, Gage FH (1990) Petit mal epilepsy and parkinsonian tremor: hypothesis of a common pacemaker. Neuroscience 36:1–14.

Connors BW, Gutnick MJ (1990) Intrinsic firing patterns of diverse neocortical neurons. Trends Neurosci 13:99–104.

Contreras D, Steriade M (1996) Spindle oscillation in cats: the role of corticothalamic feedback in a thalamically generated rhythm. J Physiol (Lond) 490:159–179.

Contreras D, Curró Dossi R, Steriade M (1993) Electrophysiological properties of cat reticular thalamic neurones *in vivo*. J Physiol (Lond) 470:273–294.

Contreras D, Destexhe A, Sejnowski TJ, Steriade M (1996) Control of spatiotemporal coherence of a thalamic oscillation by corticothalamic feedback. Science 274:771–774.

Contreras D, Destexhe A, Steriade M (1997) Intracellular and computational characterization of the intracortical inhibitory control of synchronized thalamic inputs *in vivo*. J Neurophysiol 78:335–350.

Coulter DA, Huguenard JR, Prince DA (1989) Characterization of ethosuximide reduction of low-threshold calcium current in thalamic neurons. Ann Neurol 25:582–593.

Davies CH, Davies SN, Collingridge GL (1990) Paired-pulse depression of monosynaptic GABA-mediated inhibitory postsynaptic responses in rat hippocampus. J Physiol (Lond) 424:513–531.

de la Pena E, Geijo-Barrientos E (1996) Laminar organization, morphology, and physiological properties of pyramidal neurons that have the low-threshold calcium current in the guinea pig frontal cortex. J Neurosci 16:5301–5311.

Deschênes M, Hu B (1990) Electrophysiology and pharmacology of the corticothalamic input to lateral thalamic nuclei: an intracellular study in the cat. Eur J Neurosci 2:140–152.

Destexhe A, Sejnowski TJ (1995) G-protein activation kinetics and spillover of GABA may account for differences between inhibitory responses in the hippocampus and thalamus. Proc Natl Acad Sci USA 92:9515–9519.

Destexhe A, Babloyantz A, Sejnowski TJ (1993) Ionic mechanisms for intrinsic slow oscillations in thalamic relay neurons. Biophys J 65:1538–1552.

Destexhe A, Mainen ZF, Sejnowski TJ (1994) An efficient method for computing synaptic conductances based on a kinetic model of receptor binding. Neural Comput 6:14–18.

Destexhe A, Bal T, McCormick DA, Sejnowski TJ (1996a) Ionic mechanisms underlying synchronized oscillations and propagating waves in a model of ferret thalamic slices. J Neurophysiol 76:2049–2070.

Destexhe A, Contreras D, Steriade M, Sejnowski TJ, Huguenard JR (1996b) *In vivo*, *in vitro*, and computational analysis of dendritic calcium currents in thalamic reticular neurons. J Neurosci 16:169–185.

Destexhe A, Contreras D, Steriade M (1998a) Mechanisms underlying the synchronizing action of corticothalamic feedback through inhibition of thalamic relay cells. J Neurophysiol 79:999–1016.

Destexhe A, Mainen ZF, Sejnowski TJ (1998b) Kinetic models of synaptic transmission. In: Methods in neuronal modeling, 2nd Ed (Koch C, Segev I, eds), pp 1–26. Cambridge, MA: MIT.

Dutar P, Nicoll RA (1988) A physiological role for $GABA_B$ receptors in the central nervous system. Nature 332:156–158.

Gibbs JW, Berkow-Schroeder G, Coulter DA (1996) $GABA_A$ receptor function in developing rat thalamic reticular neurons: whole cell recordings of GABA-mediated currents and modulation by clonazepam. J Neurophysiol 76:2568–2579.

Gloor P, Quesney LF, Zumstein H (1977) Pathophysiology of generalized penicillin epilepsy in the cat: the role of cortical and subcortical

structures. II. Topical application of penicillin to the cerebral cortex and subcortical structures. Electroencephalogr Clin Neurophysiol 43:79–94.
Gloor P, Pellegrini A, Kostopoulos GK (1979) Effects of changes in cortical excitability upon the epileptic bursts in generalized penicillin epilepsy of the cat. Electroencephalogr Clin Neurophysiol 46:274–289.
Golomb D, Wang XJ, Rinzel J (1996) Propagation of spindle waves in a thalamic slice model. J Neurophysiol 75:750–769.
Hersch SM, White EL (1981) Thalamocortical synapses on corticothalamic projections neurons in mouse SmI cortex: electron microscopic demonstration of a monosynaptic feedback loop. Neurosci Lett 24:207–210.
Hille B (1992) Ionic channels of excitable membranes. Sunderland, MA: Sinauer.
Hines ML, Carnevale NT (1997) The NEURON simulation environment. Neural Comput 9:1179–1209.
Hodgkin AL, Huxley AF (1952) A quantitative description of membrane current and its application to conduction and excitation in nerve. J Physiol (Lond) 117:500–544.
Hosford DA, Clark S, Cao Z, Wilson Jr WA, Lin FH, Morrisett RA, Huin A (1992) The role of $GABA_B$ receptor activation in absence seizures of lethargic (lh/lh) mice. Science 257:398–401.
Hosford DA, Wang Y, Cao Z (1997) Differential effects mediated by $GABA_A$ receptors in thalamic nuclei of lh/lh model of absence seizures. Epilepsy Res 27:55–65.
Huguenard JR, Prince DA (1994a) Clonazepam suppresses $GABA_B$-mediated inhibition in thalamic relay neurons through effects in nucleus reticularis. J Neurophysiol 71:2576–2581.
Huguenard JR, Prince DA (1994b) Intrathalamic rhythmicity studied in vitro: nominal T-current modulation causes robust anti-oscillatory effects. J Neurosci 14:5485–5502.
Inoue M, Duysens J, Vossen JMH, Coenen AML (1993) Thalamic multiple-unit activity underlying spike–wave discharges in anesthetized rats. Brain Res 612:35–40.
Jahr CE, Stevens CF (1990) A quantitative description of NMDA receptor–channel kinetic behavior. J Neurosci 10:1830–1837.
Jasper H, Kershman J (1941) Electroencephalographic classification of the epilepsies. Arch Neurol Psychiatry 45:903–943.
Kim U, Sanchez Vives MV, McCormick DA (1997) Functional dynamics of GABAergic inhibition in the thalamus. Science 278:130–134.
Kostopoulos G, Gloor P, Pellegrini A, Gotman J (1981a) A study of the transition from spindles to spike and wave discharge in feline generalized penicillin epilepsy: microphysiological features. Exp Neurol 73:55–77.
Kostopoulos G, Gloor P, Pellegrini A, Siatitsas I (1981b) A study of the transition from spindles to spike and wave discharge in feline generalized penicillin epilepsy: EEG features. Exp Neurol 73:43–54.
Kostopoulos G, Avoli M, Gloor P (1983) Participation of cortical recurrent inhibition in the genesis of spike and wave discharges in feline generalized epilepsy. Brain Res 267:101–112.
Liu XB, Honda CN, Jones EG (1995) Distribution of four types of synapse on physiologically identified relay neurons in the ventral posterior thalamic nucleus of the cat. J Comp Neurol 352:69–91.
Liu Z, Vergnes M, Depaulis A, Marescaux C (1991) Evidence for a critical role of GABAergic transmission within the thalamus in the genesis and control of absence seizures in the rat. Brain Res 545:1–7.
Liu Z, Vergnes M, Depaulis A, Marescaux C (1992) Involvement of intrathalamic $GABA_B$ neurotransmission in the control of absence seizures in the rat. Neuroscience 48:87–93.
Llinás RR (1988) The intrinsic electrophysiological properties of mammalian neurons: a new insight into CNS function. Science 242:1654–1664.
Lüthi A, McCormick DA (1998) Periodicity of thalamic synchronized oscillations: the role of Ca^{2+}-mediated upregulation of I_h. Neuron 20:553–563.
Lytton WW, Contreras D, Destexhe A, Steriade M (1997) Dynamic interactions determine partial thalamic quiescence in a computer network model of spike-and-wave seizures. J Neurophysiol 77:1679–1696.
Marcus EM, Watson CW (1966) Bilateral synchronous spike wave electrographic patterns in the cat: interaction of bilateral cortical foci in the intact, the bilateral cortical–callosal, and adiencephalic preparations. Arch Neurol 14:601–610.
McLachlan RS, Avoli M, Gloor P (1984) Transition from spindles to generalized spike and wave discharges in the cat: simultaneous single-cell recordings in the cortex and thalamus. Exp Neurol 85:413–425.
Nunez PL (1981) Electric fields of the brain: the neurophysics of EEG. Oxford: Oxford UP.
Otis TS, Mody I (1992) Modulation of decay kinetics and frequency of $GABA_A$ receptor-mediated spontaneous inhibitory postsynaptic currents in hippocampal neurons. Neuroscience 49:13–32.
Pellegrini A, Musgrave J, Gloor P (1979) Role of afferent input of subcortical origin in the genesis of bilaterally synchronous epileptic discharges of feline generalized epilepsy. Exp Neurol 64:155–173.
Pollen DA (1964) Intracellular studies of cortical neurons during thalamic induced wave and spike. Electroencephalogr Clin Neurophysiol 17:398–404.
Prevett MC, Duncan JS, Jones T, Fish DR, Brooks DJ (1995) Demonstration of thalamic activation during typical absence seizures during $H_2^{15}O$ and PET. Neurology 45:1396–1402.
Puigcerver A, Van Luijtenaar EJLM, Drinkenburg WHIM, Coenen ALM (1996) Effects of the $GABA_B$ antagonist CGP-35348 on sleep–wake states, behaviour, and spike–wave discharges in old rats. Brain Res Bull 40:157–162.
Ralston B, Ajmone-Marsan C (1956) Thalamic control of certain normal and abnormal cortical rhythms. Electroencephalogr Clin Neurophysiol 8:559–582.
Roy JP, Clercq M, Steriade M, Deschênes M (1984) Electrophysiology of neurons in lateral thalamic nuclei in cat: mechanisms of long-lasting hyperpolarizations. J Neurophysiol 51:1220–1235.
Silva LR, Amitai Y, Connors BW (1991) Intrinsic oscillations of neocortex generated by layer 5 pyramidal neurons. Science 251:432–435.
Smith KA, Fisher RS (1996) The selective $GABA_B$ antagonist CGP-35348 blocks spike–wave bursts in the cholesterol synthesis rat absence epilepsy model. Brain Res 729:147–150.
Snead OC (1992) Evidence for $GABA_B$-mediated mechanisms in experimental generalized absence seizures. Eur J Pharmacol 213:343–349.
Sodickson DL, Bean BP (1996) $GABA_B$ receptor-activated inwardly rectifying potassium current in dissociated hippocampal CA3 neurons. J Neurosci 16:6374–6385.
Steriade M (1974) Interneuronal epileptic discharges related to spike-and-wave cortical seizures in behaving monkeys. Electroencephalogr Clin Neurophysiol 37:247–263.
Steriade M, Contreras D (1995) Relations between cortical and thalamic cellular events during transition from sleep patterns to paroxysmal activity. J Neurosci 15:623–642.
Steriade M, Contreras D (1998) Spike–wave complexes and fast components of cortically generated seizures: role of neocortex and thalamus. J Neurophysiol, in press.
Steriade M, Wyzinski P, Apostol V (1972) Corticofugal projections governing rhythmic thalamic activity. In: Corticothalamic projections and sensorimotor activities (Frigyesi TL, Rinvik E, Yahr MD, eds), pp 221–272. New York: Raven.
Steriade M, Jones EG, Llinás RR (1990) Thalamic oscillations and signaling. New York: Wiley.
Steriade M, McCormick DA, Sejnowski TJ (1993) Thalamocortical oscillations in the sleeping and aroused brain. Science 262:679–685.
Thompson SM (1994) Modulation of inhibitory synaptic transmission in the hippocampus. Prog Neurobiol 42:575–609.
Thompson SM, Gahwiler BH (1992) Effects of the GABA uptake inhibitor tiagabine on inhibitory synaptic potentials in rat hippocampal slice cultures. J Neurophysiol 67:1698–1701.
Traub RD, Miles R (1991) Neuronal networks of the hippocampus. Cambridge, UK: Cambridge UP.
Tsakiridou E, Bertollini L, de Curtis M, Avanzini G, Pape HC (1995) Selective increase in T-type calcium conductance of reticular thalamic neurons in a rat model of absence epilepsy. J Neurosci 15:3110–3117.
Vergnes M, Marescaux C (1992) Cortical and thalamic lesions in rats with genetic absence epilepsy. J Neural Transm Suppl 35:71–83.
Vergnes M, Marescaux C, Micheletti G, Depaulis A, Rumbach L, Warter JM (1984) Enhancement of spike and wave discharges by GABAmimetic drugs in rats with spontaneous petit-mal-like epilepsy. Neurosci Lett 44:91–94.
von Krosigk M, Bal T, McCormick DA (1993) Cellular mechanisms of a synchronized oscillation in the thalamus. Science 261:361–364.
White EL, Hersch SM (1982) A quantitative study of thalamocortical and other synapses involving the apical dendrites of corticothalamic cells in mouse SmI cortex. J Neurocytol 11:137–157.
Williams D (1953) A study of thalamic and cortical rhythms in petit mal. Brain 76:50–69.